## SUPPLEMENTAL METHODS

**Building the UDS.** Traditional crosses were used to combine individual *CEN*-conditional chromosomes into strains with multiple centromeres marked (Supplemental Table 1 and Supplemental Fig. 1). Although each conditional chromosome contains an identical *URA3* dominant selectable marker, the segregation of these markers could be followed because of linkage to a *CEN* locus. Meiotic segregation of genetic markers tightly linked to two different centromeres generates tetrads with equal numbers of parental and nonparental ditypes (PD and NPD, respectively), while the frequency of tetratype tetrads approaches 0 (Mortimer and Hawthorne 1966). Thus for two heterozygous *CEN*-linked *URA3* markers there is equal probability of a parental configuration in which each spore contains a *URA3* marker from one parent but not the other, and a nonparental configuration in which 2 of the 4 spores contain *URA3* markers from both parents and the other 2 spores contain no marked centromeres. This probability of 1/2 can be generalized for multiple chromosomes by the equation: $P = \frac{1}{2^{n-1}}$ where n is the number of different chromosomes heterozygous for the *CEN*-linked *URA3* marker. Thus in a cross of four different heterozygous *CEN*-marked chromosomes, approximately 1 in 8 tetrads will segregate all of the *URA3* markers into 2 of the spores, and all of the unmarked chromosomes into the other two spores giving a 2:2 segregation of uracil prototrophy that is easily scored (See Supplemental Fig. 2). The segregation of *URA3* alleles in crosses with 2,3,4 or 5 *CEN*-linked markers closely followed the above prediction and were carried out with standard tetrad dissection techniques. For the higher order crosses with 8 or 16 heterozygous CEN-linked chromosomes, the probability of recovering the desired tetrads becomes 1/128 and 1/32,768 respectively. Rather than performing dissections to identify this increasingly rare segregation pattern, we sporulated the diploids and plated tetrads to generate single chimeric colonies containing the four progeny from a single meiotic event. The rare tetrads where 2 spores contain all of the *CEN*-linked *URA3* markers but the other 2 spores are uracil auxotrophs produce 5-FOA resistant colonies that are identified by replica plating. The original colony was re-streaked onto rich medium and haploid uracil prototrophs were identified by replica plating and mating tests.

Two crosses were performed to produce diploids heterozygous for conditional chromosomes 1 through 8 (strain W3199), and chromosomes 9 through 16 (strain W3200). Sporulation of strain W3199 and plating 410 tetrads produced and three 5-FOA resistant colonies. A *MAT***a** haploid strain containing conditional centromeres on chromosomes 1-8 was isolated. For strain W3200, 491 tetrads were plated and two 5-FOA-resistant strains were identified. A *MATα* haploid strain containing conditional centromeres on chromosomes 9-16 was isolated from that cross. Strains W3199 and W3200 were then crossed yielding a diploid strain heterozygous for 16 conditional chromosomes (W4730). In this tetrad screen, two 5-FOA-resistant colonies were recovered from 130,000 tetrads. Thus in each tetrad screen, the co-segregation of *CEN* markers closely followed the predicted probability.

PCR amplifications were used to confirm the presence of the *CEN*-conditional chromosomes after each round of crosses. Diagnostic amplifications were performed using primers internal to the *URA3* marker paired with chromosome specific primers distal to the centromere. For the final rounds of crosses, additional PCRs were performed across the full *CEN* region to ensure that additional untagged chromosomes (disomes) did not persist.

We isolated a *MAT***a** and a *MAT*α haploid each containing 16 conditional chromosomes. Both strains exhibited normal growth on rich or synthetic medium using glucose as a carbon source. The two strains were crossed together and sporulated to evaluate the stability of the conditional chromosomes through meiosis under permissive conditions. If centromere instability were evident, nondisjunction events during meiosis would result in spore inviability(Rockmill and Roeder 1988). Sporulation and dissection of homozygous *GAL-CEN* diploids resulted in 94% spore viability, a frequency that is typical for the W303 strain background. Therefore, under permissive conditions, the *CEN*-conditional chromosomes are stable both during meiosis and in subsequent mitotic cell divisions.

The *MAT***a** *CEN*-conditional strain (W4730-121) was transformed with plasmid pWJ1616 (a subclone of pHK256 from Hannah Klein(Fan et al. 1996) into a *TRP1* vector) for pop-in pop-out replacement of the *rad5-535* allele to make the *RAD5* strain, J1506. J1506 was subsequently transformed with a 5 kb *LYS2* DNA fragment from pRS317(Sikorski and

Hieter 1989) to make the *LYS2* strain, U2776. The *RAD5* and *LYS2* alleles were verified by phenotypic assays and sequencing. The *MAT*α *CEN*-conditional strain (W4730-257) was transformed with a 2.2 kb *ADE2* DNA fragment from pRS422(Sikorski and Hieter 1989) to make the *ADE2* strain, U2042. The *ADE2* allele in U2042 was confirmed by adenine prototrophy and sequencing. U2042 and U2776 were crossed to make strain W8164. *MAT***a** and a *MAT*α segregants were isolated to obtain universal donor strains that are *ADE2*, *LYS2* and *RAD5*.

## Supplemental Table 1. Strains.

| 1X Strains# | Genotype | Reference |
|---|---|---|
| DY6281 | *MAT**a** CEN1::pGal1-CEN1-URA3-K.lactis ade2-1 can1-100 his3-11,15 leu2-3,112 lys2 met17 trp1-1 ura3-1 rad5-535* | Reid et. al. |
| J1072 | *MATα CEN2::pGal1-CEN2-URA3-K.lactis ade2-1 can1-100 his3-11,15 leu2-3,112 lys2 met17 trp1-1 ura3-1 RAD5* | Reid et. al. |
| DY6296 | *MATα CEN3::pGal1-CEN3-URA3-K.lactis ade2-1 can1-100 his3-11,15 leu2-3,112 lys2 met17 trp1-1 ura3-1 rad5-535* | Reid et. al. |
| DY6282 | *MAT**a** CEN4::pGal1-CEN4-URA3-K.lactis ade2-1 can1-100 his3-11,15 leu2-3,112 lys2 met17 trp1-1 ura3-1 rad5-535* | Reid et. al. |
| DY6283 | *MAT**a** CEN5::pGal1-CEN5-URA3-K.lactis ade2-1 can1-100 his3-11,15 leu2-3,112 lys2 met17 trp1-1 ura3-1 rad5-535* | Reid et. al. |
| DY6300 | *MATα CEN6::pGal1-CEN6-URA3-K.lactis ade2-1 can1-100 his3-11,15 leu2-3,112 lys2 met17 trp1-1 ura3-1 rad5-535* | Reid et. al. |
| DY6301 | *MATα CEN7::pGal1-CEN7-URA3-K.lactis ade2-1 can1-100 his3-11,15 leu2-3,112 lys2 met17 trp1-1 ura3-1 rad5-535* | Reid et. al. |
| DY6302 | *MATα CEN8::pGal1-CEN8-URA3-K.lactis ade2-1 can1-100 his3-11,15 leu2-3,112 lys2 met17 trp1-1 ura3-1 rad5-535* | Reid et. al. |
| DY6287 | *MAT**a** CEN9::pGal1-CEN9-URA3-K.lactis ade2-1 can1-100 his3-11,15 leu2-3,112 lys2 met17 trp1-1 ura3-1 rad5-535* | Reid et. al. |
| DY6304 | *MATα CEN10::pGal1-CEN10-URA3-K.lactis ade2-1 can1-100 his3-11,15 leu2-3,112 lys2 met17 trp1-1 ura3-1 rad5-535* | Reid et. al. |
| DY6289 | *MAT**a** CEN11::pGal1-CEN11-URA3-K.lactis ade2-1 can1-100 his3-11,15 leu2-3,112 lys2 met17 trp1-1 ura3-1 rad5-535* | Reid et. al. |
| DY6306 | *MATα CEN12::pGal1-CEN12-URA3-K.lactis ade2-1 can1-100 his3-11,15 leu2-3,112 lys2 met17 trp1-1 ura3-1 rad5-535* | Reid et. al. |
| DY6291 | *MAT**a** CEN13::pGal1-CEN13-URA3-K.lactis ade2-1 can1-100 his3-11,15 leu2-3,112 lys2 met17 trp1-1 ura3-1 rad5-535* | Reid et. al. |
| J1073 | *MAT**a** CEN14::pGal1-CEN14-URA3-K.lactis ade2-1 can1-100 his3-11,15 leu2-3,112 lys2 met17 trp1-1 ura3-1 RAD5* | Reid et. al. |
| DY6293 | *MAT**a** CEN15::pGal1-CEN15-URA3-K.lactis ade2-1 can1-100 his3-11,15 leu2-3,112 lys2 met17 trp1-1 ura3-1 rad5-535* | Reid et. al. |
| DY6310 | *MATα CEN16::pGal1-CEN16-URA3-K.lactis ade2-1 can1-100 his3-11,15 leu2-3,112 lys2 met17 trp1-1 ura3-1 rad5-535* | Reid et. al. |
| **2X Strains$** | | |
| W3188-3C | *MATα $CEN1^{GCS}$ $CEN8^{GCS}$ ade2-1 can1-100 his3-11,15 leu2-3,112 lys2 met17 trp1-1 ura3-1 rad5-535* | this study |
| W3187-1C | *MAT**a** $CEN3^{GCS}$ $CEN4^{GCS}$ ade2-1 can1-100 his3-11,15 leu2-3,112 lys2 met17 trp1-1 ura3-1 rad5-535* | this study |
| W3189-2A | *MAT**a** $CEN5^{GCS}$ $CEN6^{GCS}$ ade2-1 can1-100 his3-11,15 leu2-3,112 lys2 met17 trp1-1 ura3-1 rad5-535* | this study |
| W3191-3B | *MAT**a** $CEN9^{GCS}$ $CEN10^{GCS}$ ade2-1 can1-100 his3-11,15 leu2-3,112 lys2 met17 trp1-1 ura3-1 rad5-535* | this study |
| W3192-1C | *MATα $CEN11^{GCS}$ $CEN12^{GCS}$ ade2-1 can1-100 his3-11,15 leu2-3,112 lys2 met17 trp1-1 ura3-1 rad5-535* | this study |
| W3193-1A | *MATα $CEN15^{GCS}$ $CEN16^{GCS}$ ade2-1 can1-100 his3-11,15 leu2-3,112 lys2 met17 trp1-1 ura3-1 rad5-535* | this study |
| **3X Strains** | | |
| W3196-19B | *MATα $CEN5^{GCS}$ $CEN6^{GCS}$ $CEN7^{GCS}$ ade2-1 can1-100 his3-11,15 leu2-3,112 lys2 met17 trp1-1 ura3-1 rad5-535* | this study |
| W3194-5A | *MATα $CEN13^{GCS}$ $CEN15^{GCS}$ $CEN16^{GCS}$ ade2-1 can1-100 his3-11,15 leu2-3,112 lys2 met17 trp1-1 ura3-1 rad5-535* | this study |
| **4X Strains** | | |
| W5748-5C | *MAT**a** $CEN1^{GCS}$ $CEN3^{GCS}$ $CEN4^{GCS}$ $CEN8^{GCS}$ ade2-1 can1-100 his3-11,15 leu2-3,112 lys2 met17 trp1-1 ura3-1 rad5-535* | this study |
| W3197-12A | *MAT**a** $CEN9^{GCS}$ $CEN10^{GCS}$ $CEN11^{GCS}$ $CEN12^{GCS}$ ade2-1 can1-100 his3-11,15 leu2-3,112 lys2 met17 trp1-1 ura3-1 rad5-535* | this study |
| W3198-2C | *MATα $CEN13^{GCS}$ $CEN14^{GCS}$ $CEN15^{GCS}$ $CEN16^{GCS}$ ade2-1 can1-100 his3-11,15 leu2-3,112 lys2 met17 trp1-1 ura3-1 rad5-535* | this study |
| **5X Strains** | | |
| W3195-19D | *MAT**a** $CEN1^{GCS}$ $CEN2^{GCS}$ $CEN3^{GCS}$ $CEN4^{GCS}$ $CEN8^{GCS}$ ade2-1 can1-100 his3-11,15 leu2-3,112 lys2 met17 trp1-1 ura3-1 rad5-535* | this study |
| **8X Strains** | | |
| W3199 | *MAT**a** $CEN1^{GCS}$ $CEN2^{GCS}$ $CEN3^{GCS}$ $CEN4^{GCS}$ $CEN5^{GCS}$ $CEN6^{GCS}$ $CEN7^{GCS}$ $CEN8^{GCS}$ ade2-1 can1-100 his3-11,15 leu2-3,112 lys2 met17 trp1-1 ura3-1 rad5-535* | this study |
| W3200 | *MATα $CEN9^{GCS}$ $CEN10^{GCS}$ $CEN11^{GCS}$ $CEN12^{GCS}$ $CEN13^{GCS}$ $CEN14^{GCS}$ $CEN15^{GCS}$ $CEN16^{GCS}$ ade2-1 can1-100 his3-11,15 leu2-3,112 lys2 met17 trp1-1 ura3-1 rad5-535* | this study |
| **16X Strains** | | |
| W4730-121 | *MAT**a** $CEN1^{GCS}$ $CEN2^{GCS}$ $CEN3^{GCS}$ $CEN4^{GCS}$ $CEN5^{GCS}$ $CEN6^{GCS}$ $CEN7^{GCS}$ $CEN8^{GCS}$ $CEN9^{GCS}$ $CEN10^{GCS}$ $CEN11^{GCS}$ $CEN12^{GCS}$ $CEN13^{GCS}$ $CEN14^{GCS}$ $CEN15^{GCS}$ $CEN16^{GCS}$ ade2-1 can1-100 his3-11,15 leu2-3,112 lys2 met17 trp1-1 ura3-1 rad5-535* | this study |
| W4730-257 | *MATα $CEN1^{GCS}$ $CEN2^{GCS}$ $CEN3^{GCS}$ $CEN4^{GCS}$ $CEN5^{GCS}$ $CEN6^{GCS}$ $CEN7^{GCS}$ $CEN8^{GCS}$ $CEN9^{GCS}$ $CEN10^{GCS}$ $CEN11^{GCS}$ $CEN12^{GCS}$ $CEN13^{GCS}$ $CEN14^{GCS}$ $CEN15^{GCS}$ $CEN16^{GCS}$ ade2-1 can1-100 his3-11,15 leu2-3,112 lys2 met17 trp1-1 ura3-1 rad5-535* | this study |
| W8164-2B | *MATα $CEN1^{GCS}$ $CEN2^{GCS}$ $CEN3^{GCS}$ $CEN4^{GCS}$ $CEN5^{GCS}$ $CEN6^{GCS}$ $CEN7^{GCS}$ $CEN8^{GCS}$ $CEN9^{GCS}$ $CEN10^{GCS}$ $CEN11^{GCS}$ $CEN12^{GCS}$ $CEN13^{GCS}$ $CEN14^{GCS}$ $CEN15^{GCS}$ $CEN16^{GCS}$ ADE2 can1-100 his3-11,15 leu2-3,112 LYS2 met17 trp1-1 ura3-1 RAD5* | this study |
| W8164-2C | *MAT**a** $CEN1^{GCS}$ $CEN2^{GCS}$ $CEN3^{GCS}$ $CEN4^{GCS}$ $CEN5^{GCS}$ $CEN6^{GCS}$ $CEN7^{GCS}$ $CEN8^{GCS}$ $CEN9^{GCS}$ $CEN10^{GCS}$ $CEN11^{GCS}$ $CEN12^{GCS}$ $CEN13^{GCS}$ $CEN14^{GCS}$ $CEN15^{GCS}$ $CEN16^{GCS}$ ADE2 can1-100 his3-11,15 leu2-3,112 LYS2 met17 trp1-1 ura3-1 RAD5* | this study |
| **Additional Strains** | | |
| W7981-2A | *MATα ADE2 his3-11,15 leu2-3,112 ura3-1 TRP1 LYS2 can1-100 RAD5* | this study |
| W5911-1A | *MATα ade2-1 his3-11,15 leu2-3,112 ura3-1 trp1-1 LYS2 can1-100 vps25Δ::KanMX RAD5* | this study |
| W9471-8C | *MATα ADE2 his3-11,15 leu2-3,112 ura3-1 TRP1 lys2Δ can1-100 RAD5* | this study |
| W8842-5C | *MATα ADE2 his3-11,15 leu2-3,112 ura3-1 TRP1 lys2Δ vps25Δ::NatMX RAD5* | this study |
| W8402-1A | *MAT**a** ADE2 leu2-3,112 his3-Δ200 ura3-52 trp1-Δ1 lys2-801 TOP1-HA-His8::HIS3 RAD5* | this study |
| EJY457 | *MAT**a** leu2-3,112 his3-Δ200 ura3-52 trp1-Δ1 lys2-801 top1-K65,91,92R-HA-His8::URA3* | Chen et. al. |
| W8646-2B | *MATα leu2-3,112 his3-Δ200 ura3-52 trp1-Δ1 lys2-801 top1-Y727F-HA-His8::HIS3* | this study |
| W8643-2D | *MAT**a** leu2-3,112 his3-Δ200 ura3-52 trp1-Δ1 lys2-801 top1-K65,91,92R,Y722F-HA-His8::HIS3* | this study |
| W8402-1C | *MATα ADE2 leu2-3,112 his3-Δ200 ura3-52 trp1-Δ1 lys2-801 TOP1-HA-His8::HIS3 vps25Δ::KanMX* | this study |
| W8402-1B | *MATα ADE2 leu2-3,112 his3-Δ200 ura3-52 trp1-Δ1 lys2-801 top1-K65,91,92R-HA-His8::URA3 vps25Δ::KanMX* | this study |
| W8646-2A | *MATα ADE2 leu2-3,112 his3-Δ200 ura3-52 trp1-Δ1 lys2-801 top1Y727F-HA-His8::HIS3 vps25Δ::KanMX* | this study |
| W8643-4A | *MAT**a** leu2-3,112 his3-Δ200 ura3-52 trp1-Δ1 lys2-801 top1-K65,91,92R,Y722F-HA-His8::HIS3 vps25Δ::KanMX* | this study |

$ For strains with more than one counter-selectable chromosome the centromere loci are abbreviated as $CENx^{GCS}$

**Supplemental Figure 1. Pedigree of universal plasmid donor strain**

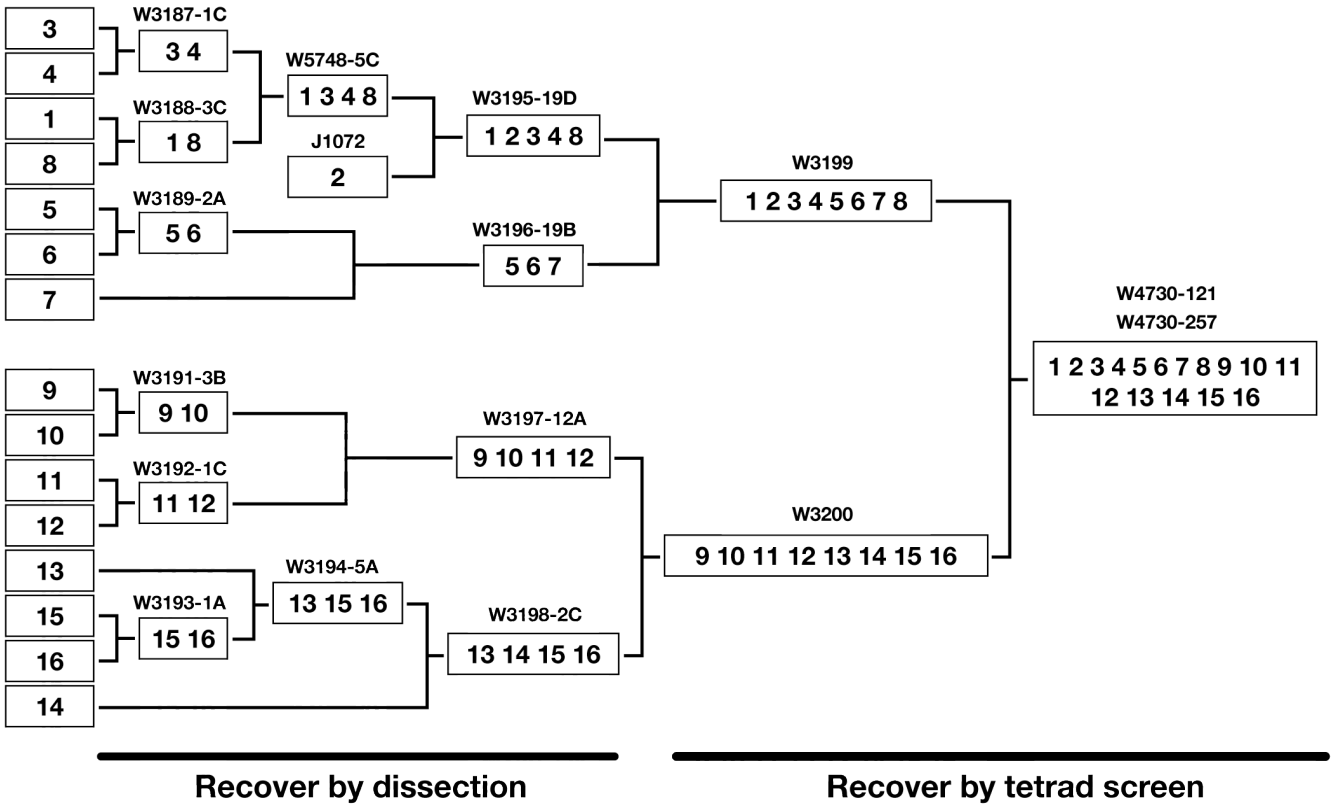


Sixteen individual strains (boxes at left), each containing a conditionally stable chromosome (numbers within boxes) were used for the pairwise crosses indicated by the lines. New strains produced are designated above the boxes. Dissections were performed to recover appropriate tetrads for the first four rounds of crosses (See Supplemental Fig. 2 for examples). A screening procedure was developed to isolate strains containing 8 and 16 conditional chromosomes (See Supplemental Methods).

**Supplemental Figure 2. Tetrad dissection to recover multiple *CEN*-marked strains**

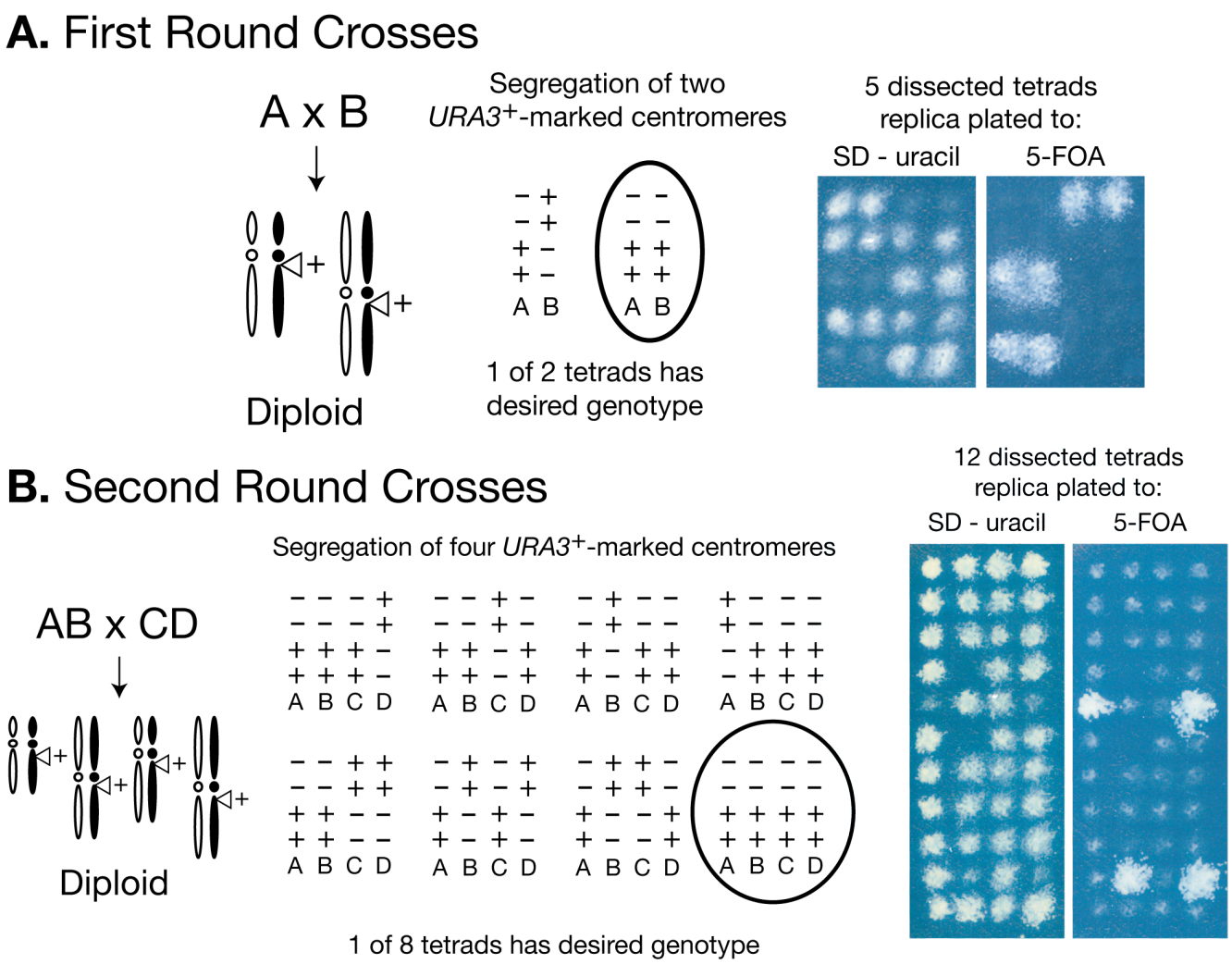


Two separate crosses and tetrad phenotypes are shown. **A.** First round crosses combined two different chromosomes (A and B) containing *CEN*-linked markers (indicated by a triangle on the chromosome icon) to make a heterozygous diploids (black and white chromosomes). *CEN*-linkage of the dominant selectable markers (*URA3*) causes it to segregate only at the reductional division in Meiosis I. Possible tetrad segregation patterns are indicated with + and - in columns marked A and B. Only two tetrad outcomes (parental ditype -PD and nonparental ditype - NPD) are possible for the first-round crosses. The *URA3* markers can segregate away from each other in meiosis I, in which case 2 spores will contain the *URA3* marker from the "A" chromosome and the other 2 spores will contain the *URA3* marker from the "B" chromosome (PD). The phenotype of

every spore is therefore the same, uracil prototrophy. The second possible outcome in meiosis I is that the two marked chromosomes segregate to the same daughter nucleus (NPD). In that case, 2 spores will each contain two copies of the *URA3* marker - one from each chromosome - while the other 2 spore will not contain any marked centromere. This second case (circled) results in a 2:2 segregation of uracil prototrophy, making the tetrads easy to identify by replica to SD-uracil medium or medium containing the drug 5-FOA to counter-select the uracil prototrophs (shown in inset). The uracil prototrophs (5-FOA sensitive) from the 2:2 tetrads were collected and verified by PCR (not show). **B.** For the second round crosses, 4 different *CEN*-linked *URA3* markers are involved, but the principle is the same. Since all four *URA3* markers segregate at meiosis I, there are 8 possible outcomes for the tetrads. One of these outcomes (circled) results in segregation of all four *CEN*-linked *URA3* markers to 2 spores and none to the other 2 spores. Again, these tetrads are easy to identify after dissection and replica to SD-uracil and 5-FOA media.

**Supplemental Figure 3. Venn diagram illustrating overlap of manual and automated data.**

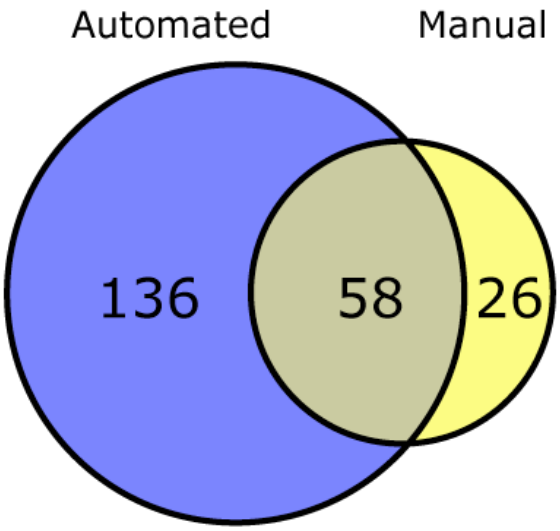


The plasmids used to screen the yeast gene disruption by the automated protocol described in the main text were also used in a manual-pin tool protocol. The donor strain, J1361 in this case, was transformed with pRS415 as a vector control, pWJ1439 for wild-type *TOP1* expression and pWJ1440 for expression of the *top1-T*$_{722}$*A* mutant. Donor strains were propagated as lawns on rich medium. The *MAT*α gene disruption library was grown in 56 different 96-well plates, then quadruplicated and transferred to agar plates having 16 by 24 grids using a 384-pin manual tool (V&P Scientific). Matings and selections were performed as described in the main text with the exception that two rounds of synthetic Gal -leu selections were used during *CEN* destabilization and 50 μM $CuSO_4$ was used to induce gene expression during the final selection step.

Analysis of growth was performed by visual inspection of digitized plate images, and the overlap of the manual pin data with the automated data sets was compared. Of the 94 strains identified as sensitive to *top1-T*$_{722}$*A* in the manual screen, 10 of these were not scored in the automated screens due to technical issues (slow growth), so comparison to the HT screens could be performed using 84 deletion strains from the manual pin screen. We used a conservative cutoff with the high throughput data and only considered strains affected by expression of the *top1-T*$_{722}$*A* mutant if they showed a significant growth effect in both automated screens. The overlap between screens is then 58 out of 84 (69%) strains

between manual and automated screens. If we further analyze the remaining 26 hits in the manual screen that are not in the high throughput dataset, we find 10 genes that are significant in one of the HT screens, but just below cutoff in the other HT screen. Relaxing the criteria to include these 10 genes increases the manual vs. HT overlap to 68 out of 84 (81%). These 10 genes are *MRC1, RVS161, OPI6, DHH1, RAD6, POL32, CBF1, VPS36, GAS1* and *MDM20*. Many of these are closely related to genes within the set shown in Table 1. We conclude that high throughput and manual pin results are closely correlated. Thus plasmid-based screens using SPA can be performed without automation or image analysis for labs that do not have access to such equipment.

**Supplemental Figure 4. Histogram showing distribution of log growth ratios for the two top1-$T_{722}$A robotic screens.**

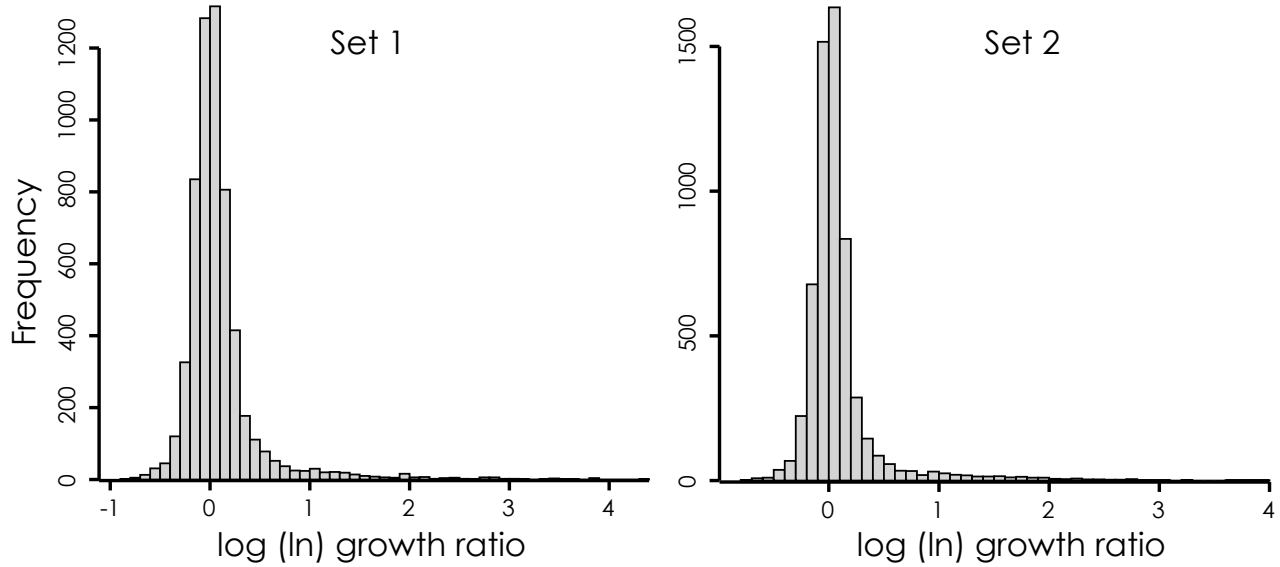


*ScreenMill* software calculates changes in growth under a particular condition, such as copper induction, by comparing growth in each strain carrying an expression plasmid, to the growth of the strain carrying an empty vector (Dittmar et al. 2010). Colony growth on each plate is first normalized to the median growth value on that plate and then the natural log of the ratio of the normalized control sample to the normalized experimental sample is calculated. The distribution of log growth ratios for an entire screen of 4827 strains approximates a normal distribution. Shown are histograms of the log growth ratios calculated in two complete screens of the gene disruption library using the *top1-$T_{722}$A* plasmid. Each distribution is centered on 0 and slow growth due to mutant expression results in a tail on the right side of the distributions. Both distributions approximate a normal curve, but show significant deviation from the normal distribution using the Lilliefors' test for normality within the nortest package in R ($p$ value < $2.2 \times 10^{-16}$)(Team 2008). Kurtosis, calculated using the moments package in R, is 27 for both distributions which indicates a peaked distribution. The $z$-score = 2 cutoff is meant as a guideline for scoring affected deletion strains. The high correlation of the two datasets combined with the approximately 85% verification (see Fig. 2 and Results) supports the use of the z = 2 cutoff.

**Supplemental Figure 5. The effect of $CuSO_4$ on the growth of the library population after SPA transfer.**

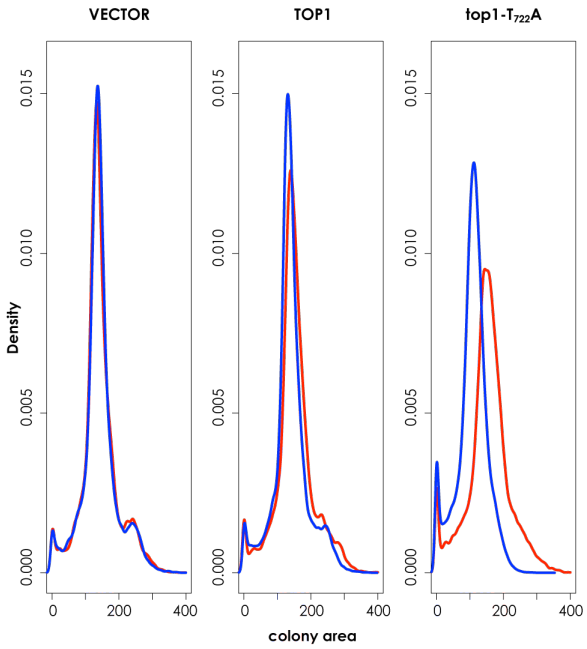


Raw growth values (*x* axes) for library strains were recorded after SPA transfer of the indicated plasmids and plotted as histograms. Growth values with (blue line) and without (red line) 100 μM $CuSO_4$ were plotted for populations containing each plasmid. Area under the curves are normalized to 1 and the *y* axis is reported as density. Strains containing a vector control and wild-type *TOP1* plasmids show no difference in the population growth average in the presence of $CuSO_4$. In contrast strains containing the *top1-T722A* mutant show slower overall growth.

**Supplemental Table 2. Auxotrophic alleles used to test chromosome loss with the Universal Donor Strain.**

| chromosome tested | allele in recipient | knockout ORF | recipient phenotype after plasmid transfer | frq. prototrophs X 10E-7 |
|---|---|---|---|---|
| 1 | *ade1* | YAR015W | ade$^-$ | 1.70 |
| 2 | *met8* | YBR213W | met$^-$ | 0.8 |
| 4 | *pet100* | YDR079W | petite | 0.4 |
| 5 | *trp2* | YER090W | trp$^-$ | 0.5 |
| 5 | *arg5,6* | YER069W | arg$^-$ | 0.3 |
| 6 | *met10* | YFR030W | met$^-$ | < 0.3 |
| 7 | *ade3* | YGR204W | ade$^-$ | < 0.3 |
| 8 | *arg4* | YHR018C | arg$^-$ | 0.4 |
| 9 | *met28* | YIR017C | met$^-$ | < 0.3 |
| 10 | *met3* | YJR010W | met$^-$ | 0.4 |
| 10 | *arg2* | YJL071W | arg$^-$ | 0.4 |
| 11 | *met14* | YKL001C | met$^-$ | 1.1 |
| 12 | *met17* | YLR303W | met$^-$ | ND |
| 13 | *ade4* | YMR300C | ade$^-$ | < 0.4 |
| 13 | *pet111* | YMR257C | petite | < 0.3 |
| 14 | *ade12* | YNL220W | ade$^-$ | 1.1 |
| 14 | *pet494* | YNR045W | petite | < 0.3 |
| 15 | *ade2* | YOR128C | ade$^-$ | < 0.3 |
| 15 | *arg1* | YOL058W | arg$^-$ | 1.0 |
| 16 | *met16* | YPR167C | met$^-$ | 0.3 |
| 1, 5, 7, 10, 13 | *ade1, his1, lys7, met3, trp5* | NA | ade$^-$, his$^-$, lys$^-$, met$^-$, trp$^-$ | ND |

*MATα* library strains containing auxotrophic deletion alleles were tested after transfer of the pWJ1512 empty vector plasmid using the SPA protocol. The strains are listed by the chromosome number of the deletion allele. For each diploid, after SPA, cells containing the transferred plasmid were recovered that were *MATα* and auxotrophic for the deletion allele, indicating that markers on at least two separate chromosomes were simultaneously lost. Next, those selected plasmid bearing cells were resuspended and plated on dropout medium to determine the frequency of prototrophic papillae, which estimates the gene conversion frequency of the *CEN*-linked *URA3* allele on the indicated chromosome. The results show that the frequency of background prototrophs is very small ($1.7 \times 10^{-7}$ or lower). The final strain in the list (K396-22B, a gift from Sue Klapholz) was used to show that five markers on different chromosomes, which are complemented in the diploid, are simultaneously recovered as auxotrophs after the SPA protocol.

**Supplemental Table 3. The number of observed vs. the number of expected mutants identified per chromosome**

| Chromosome | ORFs assayed | observed | expected | *p* value* | Significant |
|---|---|---|---|---|---|
| **I** | 75 | 7 | 3 | 0.33 | no |
| **II** | 318 | 12 | 14 | 0.84 | no |
| **III** | 136 | 7 | 6 | 1.00 | no |
| **IV** | 579 | 32 | 26 | 0.50 | no |
| **V** | 206 | 7 | 9 | 0.80 | no |
| **VI** | 93 | 2 | 4 | 0.68 | no |
| **VII** | 407 | 14 | 18 | 0.59 | no |
| **VIII** | 185 | 10 | 8 | 0.81 | no |
| **IX** | 162 | 3 | 7 | 0.34 | no |
| **X** | 272 | 12 | 12 | 1.00 | no |
| **XI** | 248 | 7 | 11 | 0.47 | no |
| **XII** | 390 | 17 | 17 | 1.00 | no |
| **XIII** | 387 | 19 | 17 | 0.86 | no |
| **XIV** | 305 | 16 | 14 | 0.85 | no |
| **XV** | 434 | 21 | 19 | 0.87 | no |
| **XVI** | 366 | 18 | 16 | 0.86 | no |
| **totals** | 4563 | 204 | | | |

4563 unique ORF deletions were analyzed that produced measurable growth data in both experiments. 204 ORFs (listed in Table 1) showed a significant growth defect upon expression of the *top1-T722A* mutant giving an average "hit" frequency of 1 in 22.4 ORFs. We calculated the expected number of hits for each chromosome based on this frequency and found no significant deviation from the expected value.

* *p* values were calculated using Fisher's exact test with a 2-tailed distribution.

**Supplemental Figure 6. Verification by plasmid transformation.**

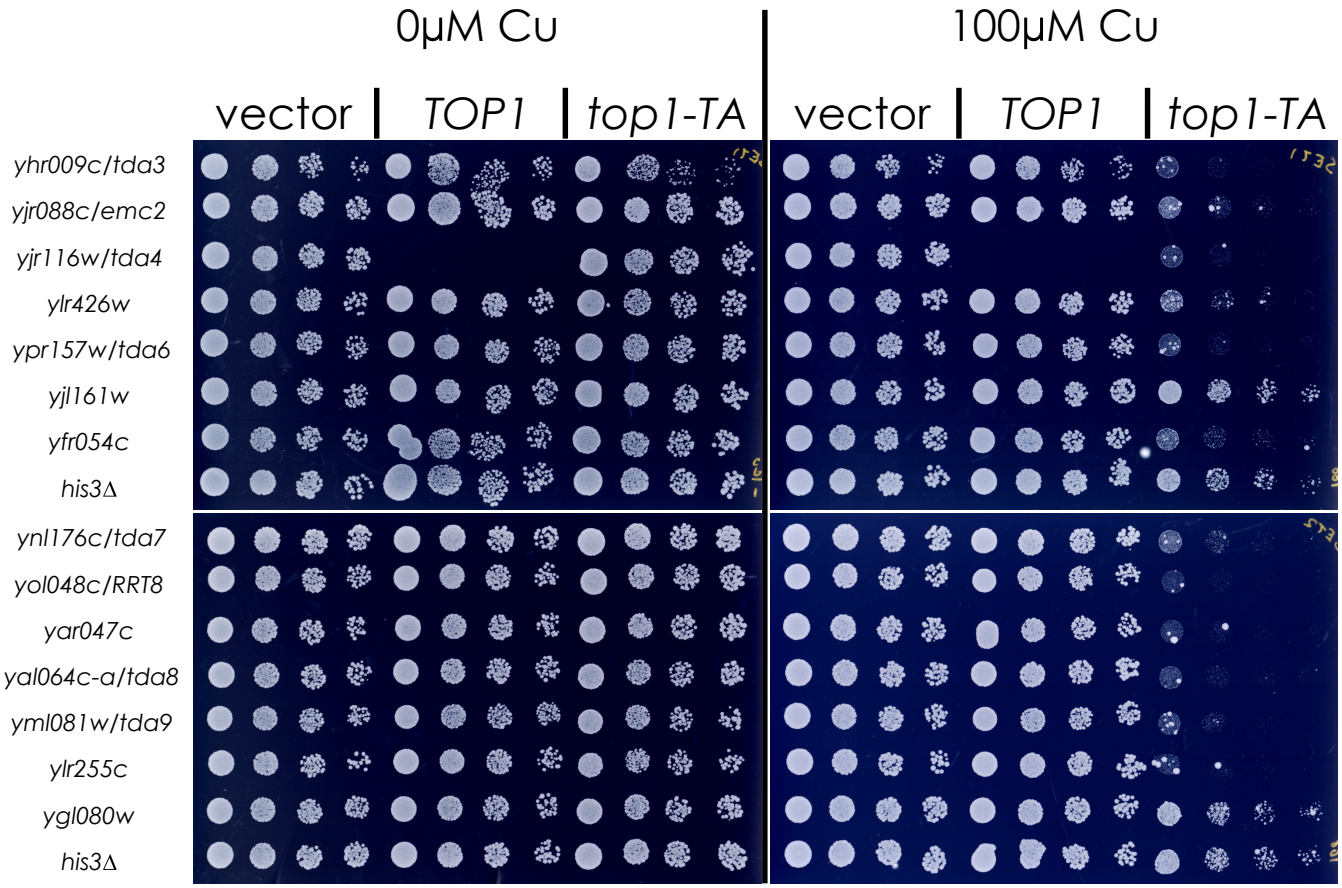


Fourteen uncharacterized strains showing a significant sensitivity to expression of *top1-$T_{722}A$* from the SPA screens were individually transformed with vector control, wild-type *TOP1* or *top1-$T_{722}A$* expression plasmids. Transformants were grown and serial dilutions were spotted onto SD-leu media with or without 100 μM $CuSO_4$. Twelve of the fourteen strains showed sensitivity to *top1-$T_{722}A$* expression in these individual experiments. The *yjr116w* mutant strain was not transformed with *TOP1* for this experiment, so those positions are blank. Seven of the ORFs shown here were renamed *TDA*, for Top1-TA dosage affected (see Results).

**Supplemental Table 4. GO term enrichment for the set of 190 genes**

| GO Process | *p* value |
|---|---|
| GO:0006974 response to DNA damage stimulus | 9.30E-18 |
| GO:0006302 double-strand break repair | 3.60E-16 |
| GO:0006259 DNA metabolic process | 3.60E-16 |
| GO:0006310 DNA recombination | 7.10E-16 |
| GO:0034984 cellular response to DNA damage stimulus | 5.30E-14 |
| GO:0006281 DNA repair | 5.70E-14 |
| GO:0016197 endosome transport | 9.90E-13 |
| GO:0006950 response to stress | 2.80E-11 |
| GO:0006996 organelle organization | 5.50E-11 |
| GO:0000725 recombinational repair | 2.30E-10 |
| GO:0000726 non-recombinational repair | 4.30E-10 |
| GO:0051052 regulation of DNA metabolic process | 9.50E-10 |
| GO:0000724 double-strand break repair via homologous recombination | 1.70E-09 |
| GO:0007034 vacuolar transport | 2.30E-09 |
| GO:0000279 M phase | 2.70E-09 |
| GO:0022403 cell cycle phase | 3.90E-09 |
| GO:0050896 response to stimulus | 4.10E-09 |
| GO:0051276 chromosome organization | 1.10E-08 |
| GO:0065008 regulation of biological quality | 1.60E-08 |
| GO:0043285 biopolymer catabolic process | 1.80E-08 |
| GO:0051716 cellular response to stimulus | 2.30E-08 |
| GO:0022402 cell cycle process | 2.40E-08 |
| GO:0007049 cell cycle | 2.40E-08 |
| GO:0006312 mitotic recombination | 3.70E-08 |
| GO:0042147 retrograde transport, endosome to Golgi | 3.80E-08 |
| GO:0065007 biological regulation | 6.50E-08 |
| GO:0031570 DNA integrity checkpoint | 9.30E-08 |
| GO:0007064 mitotic sister chromatid cohesion | 9.60E-08 |
| GO:0033554 cellular response to stress | 1.00E-07 |
| GO:0009987 cellular process | 1.50E-07 |
| GO:0044265 cellular macromolecule catabolic process | 2.50E-07 |
| GO:0007127 meiosis I | 3.10E-07 |
| GO:0007059 chromosome segregation | 3.20E-07 |
| GO:0006303 double-strand break repair via nonhomologous end joining | 4.10E-07 |
| GO:0000722 telomere maintenance via recombination | 5.60E-07 |
| GO:0051053 negative regulation of DNA metabolic process | 5.90E-07 |
| GO:0009057 macromolecule catabolic process | 6.10E-07 |
| GO:0045053 protein retention in Golgi apparatus | 7.70E-07 |
| GO:0000727 double-strand break repair via break-induced replication | 9.80E-07 |
| GO:0045003 double-strand break repair via synthesis-dependent strand annealing | 9.80E-07 |

| GO Cellular Component | *p* value |
|---|---|
| GO:0005768 endosome | 7.20E-12 |
| GO:0030904 retromer complex | 1.90E-08 |
| GO:0043234 protein complex | 4.40E-08 |
| GO:0005694 chromosome | 8.10E-08 |
| GO:0044440 endosomal part | 1.80E-07 |
| GO:0043227 membrane-bounded organelle | 4.80E-07 |
| GO:0043231 intracellular membrane-bounded organelle | 4.80E-07 |
| GO:0043229 intracellular organelle | 8.40E-07 |
| GO:0043226 organelle | 8.60E-07 |

The set of 191 genes sensitive to *top1-$T_{722}$A* expression were analyzed for GO term enrichment using AMIGO (http://amigo.geneontology.org/).

**Comparison to SGA-based plasmid transfer.** We compared screening by plasmid transfer with the SPA protocol to screening by plasmid transfer with SGA. The empty vector and the *top1-T722A* expression vectors were transformed into the *MATα* SPA donor and the *MATα* SGA donor strain (See Methods) before mating to 1044 strains in the *MAT***a** gene disruption library. After plasmid transfer, plates were replica-pinned to plates containing $CuSO_4$ to induce gene expression and allowed to grow for 2 days before scanning. Images from both screens were analyzed using *ScreenMill* software. The SPA screen identified 42 of the 1044 strains screened showing significant sensitivity to *top1-T722A* expression, while the SGA screen identified 40. Eighteen deletions were identified in both screens, showing a significant overlap in these 2 screen protocols (Hypergeometric statistic $P(18) = 8 \times 10^{-17}$). A complete list of the genes identified in each miniscreen is shown in Supplemental Table 5 below. We found a similar level of overlap when comparing gene deletions identified as showing synthetic lethality or synthetic sickness with *sgs1*Δ by the SGA and dSLAM methods (Pan et al. 2006; Tong et al. 2004). In that case 36 and 65 genetic interactions were identified with an overlapping set of 17 genes (Hypergeometric statistic $P(17) = 2 \times 10^{-23}$).

**Supplemental Table 5. Deletion strains identified as sensitive to *top1-T722A* expression after SPA or SGA assisted plasmid transfer.**

| SPA protocol | | | | SGA protocol | | | |
|---|---|---|---|---|---|---|---|
| ***p* value** | ***z* score** | **ORF** | **GENE** | ***p* value** | ***z* score** | **ORF** | **GENE** |
| 9.83E-16 | 8.03 | YML032C | ***RAD52*** | 8.83E-15 | 7.76 | YLL002W | ***RTT109*** |
| 1.51E-11 | 6.75 | YOR080W | ***DIA2*** | 5.24E-12 | 6.90 | YDR076W | ***RAD55*** |
| 3.95E-11 | 6.61 | YDR076W | ***RAD55*** | 1.39E-10 | 6.42 | YML032C | ***RAD52*** |
| 5.78E-11 | 6.55 | YDR386W | *MUS81* | 7.31E-10 | 6.16 | YDR369C | ***XRS2*** |
| 9.68E-10 | 6.11 | YLL002W | ***RTT109*** | 6.77E-08 | 5.40 | YMR179W | ***SPT21*** |
| 1.84E-09 | 6.01 | YNL273W | ***TOF1*** | 1.38E-06 | 4.83 | YOR080W | ***DIA2*** |
| 4.30E-09 | 5.87 | YAR002W | ***NUP60*** | 4.05E-06 | 4.61 | YOL076W | *MDM20* |
| 8.85E-08 | 5.35 | YDR369C | ***XRS2*** | 5.57E-05 | 4.03 | YDR392W | *SPT3* |
| 1.28E-06 | 4.84 | YMR190C | ***SGS1*** | 9.21E-05 | 3.91 | YBR224W | ***YBR224W*** |
| 1.75E-05 | 4.29 | YLR061W | *RPL22A* | 2.23E-04 | 3.69 | YOR061W | *CKA2* |
| 2.39E-05 | 4.22 | YLR119W | *SRN2* | 2.65E-04 | 3.65 | YNL273W | ***TOF1*** |
| 2.90E-05 | 4.18 | YLR074C | *BUD20* | 5.37E-04 | 3.46 | YDR075W | *PPH3* |
| 6.45E-05 | 4.00 | YBR264C | *YPT10* | 5.70E-04 | 3.45 | YOR368W | ***RAD17*** |
| 1.97E-04 | 3.72 | YLR081W | *GAL2* | 7.31E-04 | 3.38 | YMR190C | ***SGS1*** |
| 2.14E-04 | 3.70 | YLR062C | *BUD28* | 1.20E-03 | 3.24 | YBR209W | *YBR209W* |
| 2.54E-04 | 3.66 | YMR198W | ***CIK1*** | 1.84E-03 | 3.11 | YAR002W | ***NUP60*** |
| 6.76E-04 | 3.40 | YAL034C | *FUN19* | 2.09E-03 | 3.08 | YPL192C | *PRM3* |

| | | | | | | | |
|---|---|---|---|---|---|---|---|
| 1.11E-03 | 3.26 | YOR078W | *BUD21* | 2.59E-03 | 3.01 | YMR039C | *SUB1* |
| 1.36E-03 | 3.20 | YNL291C | ***MID1*** | 2.65E-03 | 3.01 | YPL256C | *CLN2* |
| 2.92E-03 | 2.98 | YBR224W | ***YBR224W*** | 2.99E-03 | 2.97 | YBR223C | *TDP1* |
| 5.89E-03 | 2.75 | YEL003W | *GIM4* | 3.55E-03 | 2.92 | YMR198W | ***CIK1*** |
| 6.19E-03 | 2.74 | YPL205C | ***YPL205C*** | 4.70E-03 | 2.83 | YDR378C | ***LSM6*** |
| 7.00E-03 | 2.70 | YMR179W | ***SPT21*** | 8.04E-03 | 2.65 | YLR079W | *SIC1* |
| 7.71E-03 | 2.66 | YEL059W | *YEL059W* | 8.46E-03 | 2.63 | YLR087C | ***CSF1*** |
| 8.03E-03 | 2.65 | YNL248C | *RPA49* | 8.50E-03 | 2.63 | YPL103C | *YPL103C* |
| 0.013 | 2.49 | YML008C | *ERG6* | 9.42E-03 | 2.60 | YPL152W | *RRD2* |
| 0.013 | 2.48 | YDR378C | ***LSM6*** | 0.011 | 2.53 | YPL205C | ***YPL205C*** |
| 0.016 | 2.40 | YLL040C | *VPS13* | 0.012 | 2.50 | YAL019W | *FUN30* |
| 0.016 | 2.40 | YOR068C | *VAM10* | 0.014 | 2.46 | YNL291C | ***MID1*** |
| 0.017 | 2.38 | YLR087C | ***CSF1*** | 0.014 | 2.45 | YBR175W | *SWD3* |
| 0.018 | 2.37 | YOR293W | *RPS10A* | 0.015 | 2.43 | YDR110W | *FOB1* |
| 0.018 | 2.36 | YLR056W | *ERG3* | 0.016 | 2.41 | YPL261C | *YPL261C* |
| 0.021 | 2.32 | YOR033C | *EXO1* | 0.026 | 2.22 | YLL043W | *FPS1* |
| 0.021 | 2.31 | YDR126W | *SWF1* | 0.029 | 2.19 | YDR139C | *RUB1* |
| 0.022 | 2.28 | YAL002W | *VPS8* | 0.029 | 2.18 | YOR025W | *HST3* |
| 0.024 | 2.26 | YBR267W | *REI1* | 0.031 | 2.16 | YEL066W | *HPA3* |
| 0.026 | 2.23 | YDR067C | *YDR067C* | 0.034 | 2.13 | YAL013W | ***DEP1*** |
| 0.030 | 2.18 | YPL234C | *TFP3* | 0.036 | 2.10 | YDR435C | ***PPM1*** |
| 0.030 | 2.17 | YEL015W | *EDC3* | 0.040 | 2.05 | YDR078C | *SHU2* |
| 0.031 | 2.16 | YOR368W | ***RAD17*** | 0.042 | 2.04 | YMR003W | *YMR003W* |
| 0.032 | 2.14 | YAL013W | ***DEP1*** | | | | |
| 0.038 | 2.08 | YDR435C | ***PPM1*** | | | | |

Bold indicates deletion strains identified in SPA and SGA screens. Deletion of the *YBR224W* ORF partially deletes the *TDP1* gene. Deletion of the *YPL205C* ORF deletes the promoter region of the essential gene *HRR25*.

**Supplemental Figure 7. *CUP1* promoter function in mutant strains**

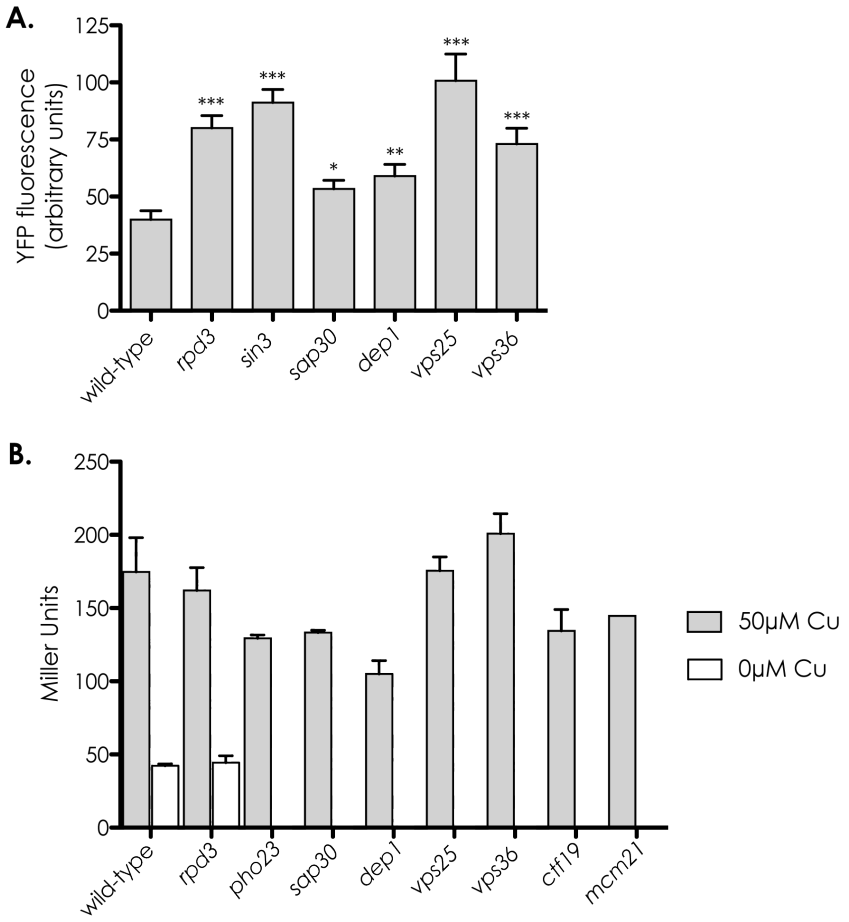


**A.** Seven strains from the yeast gene disruption collection were transformed with a plasmid bearing an N-terminal *YFP-TOP1* fusion (pWJ1546) to measure Top1 levels using fluorescence microscopy. Overnight cultures of transformants were prepared for microscopic analysis as in the METHODS section, except that 50 μM $CuSO_4$ was used to induce expression prior to microscopic analysis. Bars represent mean fluorescence intensity for 50 or more cells of the indicated strains. The *his3* mutant strain is unaffected in the *top1-$T_{722}$A* SPA screen and serves as a 'wild-type' control for the microscopic analysis. Mean values were compared to wild-type using student's *t* test; * indicates $p$ <0.05, ** indicates $p < 0.01$, *** indicates $p < 0.0001$. **B.** The same strains shown in panel A were also transformed with the beta-galactosidase gene cloned under the control of the *CUP1* promoter (pWJ1602). Transformants were grown to mid-log phase in SC-leu medium and copper sulfate was added to either 0 or 50 μM final concentration. After 4 hours cells were collected and beta-galactosidase activity was measured using the Pierce

assay kit (Rockford, IL). Uninduced controls were performed in the *rpd3* and *his3* strains to measure basal expression. Copper induction results in a 3- to 4-fold induction of beta-galactosidase activity in all of the strains showing that expression from the *CUP1* promoter is similar in each of these strains.

**Supplemental Figure 8. *YFP-TOP1* expression in kinetochore mutant strains**

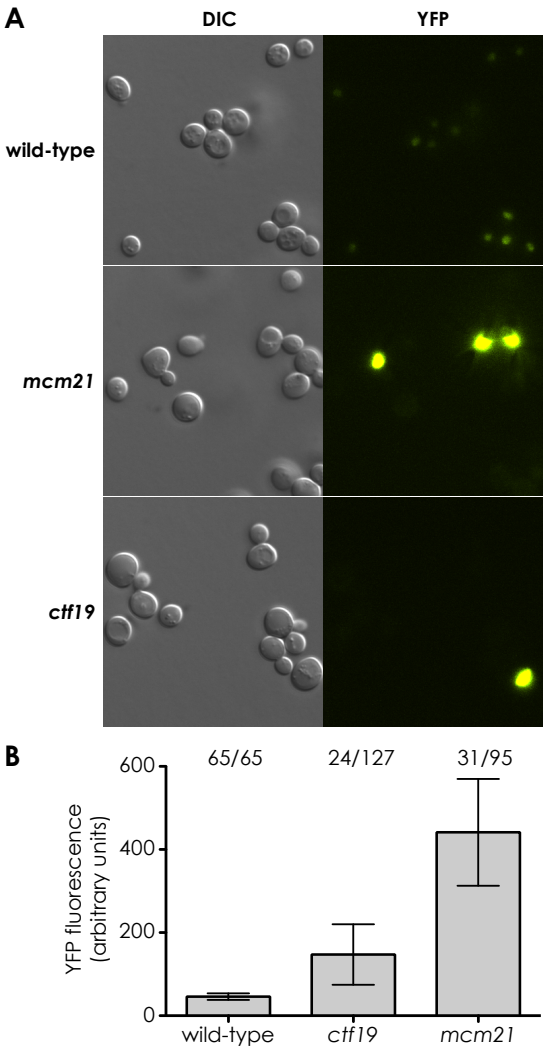


**A.** Wild-type or *mcm21* and *ctf19* mutant strains were transformed with YFP-TOP1 (pWJ1546) and imaged as described in Fig. S7 above. Wild-type strains show YFP signal from Top1 in every cell in the field. In contrast, the kinetochore mutant strains *mcm21* and *ctf19* show a large amount of fluorescence in just a few cells in the field. **B.** Fluorescent signals from images in A were quantified as described in METHODS. Bars represent mean fluorescence signal (arbitrary units) and error bars show 95% confidence intervals. Numbers above the bars indicate the number of cells from the DIC images that showed fluorescence, and mean signal was calculated only from the cells having a signal. This phenotype is consistent with a kinetochore defect where the plasmid is not efficiently transmitted to daughter cells. Plasmid buildup in mother cells would then account for amplified signal in a few strains.

**Bibliography**

Chen, X.L., Silver, H.R., Xiong, L., Belichenko, I., Adegite, C., and Johnson, E.S. 2007. Topoisomerase I-dependent viability loss in *Saccharomyces cerevisiae* mutants defective in both SUMO conjugation and DNA repair. *Genetics* **177:** 17-30.

Dittmar, J.C., Reid, R.J., and Rothstein, R. 2010. *ScreenMill*: A freely available software suite for growth measurement, analysis and visualization of high-throughput screen data. *BMC Bioinformatics* **11:** 353.

Fan, H.Y., Cheng, K.K., and Klein, H.L. 1996. Mutations in the RNA polymerase II transcription machinery suppress the hyperrecombination mutant *hpr1* delta of *Saccharomyces cerevisiae*. *Genetics* **142:** 749-759.

Mortimer, R.K. and Hawthorne, D.C. 1966. Genetic mapping in *Saccharomyces*. *Genetics* **53:** 165-173.

Pan, X., Ye, P., Yuan, D.S., Wang, X., Bader, J.S., and Boeke, J.D. 2006. A DNA integrity network in the yeast *Saccharomyces cerevisiae*. *Cell* **124:** 1069-1081.

Reid, R.J., Sunjevaric, I., Voth, W.P., Ciccone, S., Du, W., Olsen, A.E., Stillman, D.J., and Rothstein, R. 2008. Chromosome-scale genetic mapping using a set of 16 conditionally stable *Saccharomyces cerevisiae* chromosomes. *Genetics* **180:** 1799-1808.

Rockmill, B. and Roeder, G.S. 1988. *RED1*: a yeast gene required for the segregation of chromosomes during the reductional division of meiosis. *Proc. Natl. Acad. Sci. U S A* **85:** 6057-6061.

Sikorski, R.S. and Hieter, P. 1989. A system of shuttle vectors and yeast host strains designed for efficient manipulation of DNA in *Saccharomyces cerevisiae*. *Genetics* **122:** 19-27.

Team, R. 2008. R: A language and environment for statistical computing. *R Foundation for Statistical Computing Vienna Austria* ….

Tong, A.H., Lesage, G., Bader, G.D., Ding, H., Xu, H., Xin, X., Young, J., Berriz, G.F., Brost, R.L., Chang, M. et al. 2004. Global mapping of the yeast genetic interaction network. *Science* **303:** 808-813.